Interferometric Photonic Crystal Modulators with Lithium Niobate

Hugo Larocque,^{1,*} Alexander Sludds,¹ Hamed Sattari,² Ian Christen,¹ Dashiell L.P. Vitullo,³ Amir H. Ghadimi,² Dirk Englund,¹ Mikkel Heuck⁴

¹Research Laboratory of Electronics, Massachusetts Institute of Technology, Cambridge, MA 02139, USA
²Centre Suisse d'Electronique et de Microtechnique (CSEM), 2000 Neuchâtel, Switzerland
³ DEVCOM Army Research Laboratory, Adelphi, MD 20783-1193, USA
⁴ Department of Electrical and Photonics Engineering, Technical University of Denmark, 2800 Lyngby, Denmark
*hlarocqu@mit.edu

Abstract: We demonstrate a photonic crystal cavity interferometric modulator in thin-film lithium niobate on insulator with 6 GHz bandwidth, 35 dB extinction, $2\pi \times 1.27$ GHz/V DC-tuning, and a 40-by-200 micron square footprint. © 2023 The Author(s)

Chip-scale optical modulation is emerging as a disruptive route towards scalable solutions for applications ranging from quantum information processing to optical communications. Photonic integrated circuits (PICs) implemented in thin-film lithium niobate (TFLN) are of particular interest to those tasks [1] as its strong electro-optic coefficient leads to modulation rates exceeding tens of GHz while operating at CMOS voltages [2]. With wafer-scale TFLN photonics fabrication processes now available [3], larger-scale devices relying on multiple modulators have distinguished themselves as viable solutions for problems involving optical control [4]. However, the length of these devices are in the mm range in typical Mach-Zehnder configurations [2], and this limits the number of modulation channels per chip area. Cavity-based modulation has been investigated to address this issue [5]. Namely, electro-optically shifting the resonant frequency of an optical cavity can drastically affect optical transmission. However, achieving large extinction ratios in two-sided nanobeam cavity structures [5] is challenging due to the slow fall-off of their Lorentzian lineshape.

To address these problems, we propose an interferometric TFLN modulator relying on two active photonic crystal cavities. Figure 1(a) illustrates our design concept that is based on a Michelson interferometer configuration with two arms terminated by one-sided Fabry-Perot cavities. Figure 1(b) shows an optical micrograph of our PIC implementation consisting of a 50/50 directional coupler and two one-sided photonic crystal (PhC) cavities. The inset depicts a scanning electron microscope image of the PhC Bragg-reflector, which is longer on the left hand side to ensure the cavity is one-sided. Three electrodes are used to independently control the resonances of the two cavities via the electro-optic effect, $\omega_n = \omega_{0,n} + \partial_V \omega \times V_n$, where V_n is the voltage applied to the electrodes as illustrated in Fig. 1(b). From coupled-mode theory, the transmission coefficient of the device, $t_{\rm MI}(\omega)$, is:

$$t_{\text{MI}}(\boldsymbol{\omega}) = i \left(r_1(\boldsymbol{\omega}) + r_2(\boldsymbol{\omega}) \right) \zeta \sqrt{1 - \zeta^2}, \qquad r_n(\boldsymbol{\omega}) = 1 - \frac{\kappa_{c,n}}{i \delta_n + \kappa_{c,n}/2 + \kappa_{i,n}/2}, \tag{1}$$

where ζ^2 is the power splitting ratio of the directional coupler, $r_n(\omega)$ is the reflection coefficient of a one-sided cavity with detuning $\delta_n = \omega_n - \omega$, coupling rate $\kappa_{c,n}$, intrinsic loss rate $\kappa_{i,n}$, and total linewidth $\kappa_n = \kappa_c + \kappa_i$. For overcoupled cavities ($\kappa_{c,n} > \kappa_{i,n}$), the phase of $r_n(\omega)$ varies by 2π as the frequency is swept across the resonance.

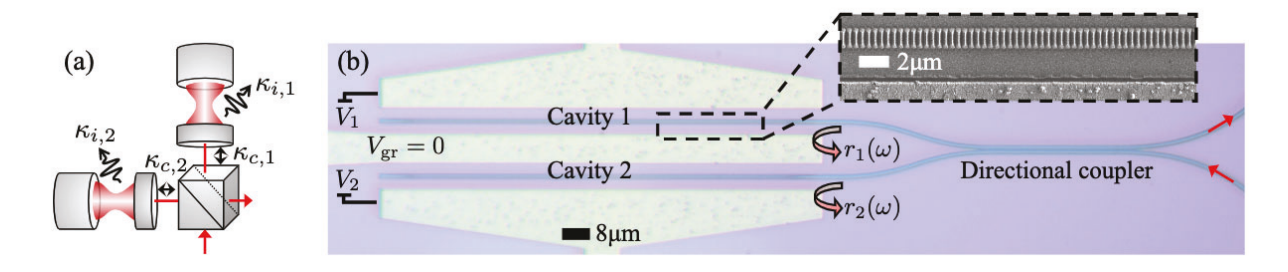


Fig. 1. (a) Schematic of our Michelson-interferometer configuration where two output arms of a 50/50 beamsplitter are terminated with one-sided cavities. (b) Optical micrograph of the fabricated device showing the three electrodes (yellow) used to control the resonance frequency of the cavities. The inset shows a scanning electron microscope image of a part of the photonic crystal cavity.

Adjusting the detuning of each cavity using voltages V_1 and V_2 allows full control of both phase and amplitude of the modulator transmission, $t_{\rm MI}$. Complete extinction ($t_{\rm MI}=0$) is possible for any value of ζ as seen from Eq. (1). Only the insertion loss is negatively affected if the splitting ratio of the directional coupler is not exactly 50/50.

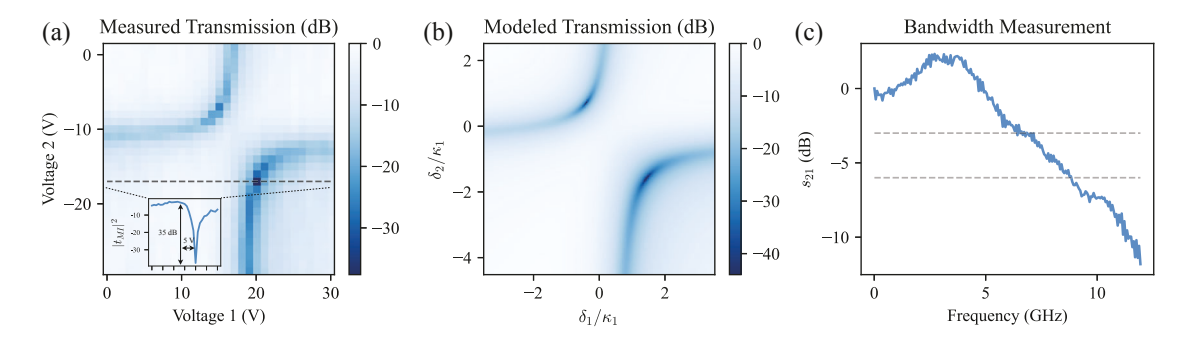


Fig. 2. (a) Measured intensity transmission as a function of DC bias voltage on each electrode. The inset shows the transmission along the cross-section indicated with a dashed line. (b) Plot of $|t_{\rm MI}(\delta_1, \delta_2)|^2$ from Eq. (1). The parameters used are: $\kappa_{c,1}/\kappa_1 = 2.0$, $\kappa_{c,1}/\kappa_{i,1} = 5.7$, $\kappa_{c,2}/\kappa_1 = 1.7$, $\kappa_{c,2}/\kappa_{i,2} = 3.9$, $\kappa_2/\kappa_1 = 1$, and $\zeta = 1/\sqrt{2}$. (c) Measured small-signal response of the device.

Our devices are fabricated using electron-beam lithography and a partial etch of 400 nm in a 600 nm thick lithium niobate membrane with air cladding on the top and SiO_2 cladding on the bottom. The electrodes are defined in a 600 nm thick gold layer.

Figure 2(a) shows measurements of the transmission as a function of V_1 and V_2 with the laser wavelength fixed at $\lambda=1558$ nm and polarization set to couple into the TEO mode of the TFLN waveguide. The resulting transmission map is in good agreement with our coupled mode theory model, shown in Fig. 2(b). Two branches of transmission dips are observed, each corresponding to one of the cavities. When the resonances approach each other, an avoided crossing is observed in the spectrum. The local minima in each branch is attributed to perfect destructive interference between the signals reflected from the photonic crystals at the output of the directional coupler. The inset in Fig. 2(a) highlights that an extinction ratio of 34 dB is possible when varying the voltage across one of the cavities by 5 V. We extract the tuning efficiency, $\partial_V \omega = 2\pi \times 1.27$ GHz/V, by scanning the laser wavelength across the resonance of each cavity and tracking the resonance location as a function of applied DC voltage. The quality factor of the cavities are estimated to be $Q_{c,1} = 3.5 \times 10^4$, $Q_{i,1} = 2.0 \times 10^5$, $Q_{c,2} = 4.1 \times 10^4$, and $Q_{i,2} = 1.6 \times 10^5$ from transmission spectra taken with a large separation between ω_1 and ω_2 .

The modulation bandwidth of our modulator is measured using a vector network analyzer. Here, the laser wavelength was again fixed close to the resonance of cavity 1 while a sinusoidal signal was added to the DC offset of V_1 . Figure 2(c) plots the small-signal response and a 3 dB cutoff of \sim 6 GHz is observed. The modulation speed is limited by the cavity decay rates ($\kappa_1 = 2\pi \times 6.4$ GHz, and $\kappa_2 = 2\pi \times 5.9$ GHz), which matches well with the cutoff frequency.

In summary, we introduce an integrated device for compact optical modulation in a TFLN photonics platform. Compared to standard MZI TFLN modulators [2], the one presented here performs with a minor sacrifice in bandwidth and actuation voltage for significant gains in device footprint. Such interferometric cavity-assisted devices provide a promising route towards integrating a large number of on-chip photonic modulation channels, with applications ranging from coherent communications to quantum control.

References

- 1. D. Zhu et al., "Integrated photonics on thin-film lithium niobate," Adv. Opt. Photonics 13, 242–352 (2021).
- 2. C. Wang et al., "Integrated lithium niobate electro-optic modulators operating at CMOS-compatible voltages," Nature **562**, 101–104 (2018).
- 3. K. Luke et al., "Wafer-scale low-loss lithium niobate photonic integrated circuits," Opt. Express 28, 24452–24458 (2020).
- 4. I. Christen et al., "An integrated photonic engine for programmable atomic control," arXiv preprint arXiv:2208.06732 (2022).
- 5. M. Li et al., "Lithium niobate photonic-crystal electro-optic modulator," Nat. Commun. 11, 4123 (2020).